



# Calculation of river sediment fluxes from uncertain and infrequent measurements

B. Cheviron, Magalie Delmas, Olivier Cerdan, J.M. Mouchel

## ► To cite this version:

B. Cheviron, Magalie Delmas, Olivier Cerdan, J.M. Mouchel. Calculation of river sediment fluxes from uncertain and infrequent measurements. *Journal of Hydrology*, 2014, 508, pp.364-373. 10.1016/j.jhydrol.2013.10.057 . hal-01098277

**HAL Id: hal-01098277**

**<https://hal.science/hal-01098277>**

Submitted on 23 Dec 2014

**HAL** is a multi-disciplinary open access archive for the deposit and dissemination of scientific research documents, whether they are published or not. The documents may come from teaching and research institutions in France or abroad, or from public or private research centers.

L'archive ouverte pluridisciplinaire **HAL**, est destinée au dépôt et à la diffusion de documents scientifiques de niveau recherche, publiés ou non, émanant des établissements d'enseignement et de recherche français ou étrangers, des laboratoires publics ou privés.

**Calculation of river sediment fluxes from uncertain and infrequent measurements**

Bruno Cheviron<sup>1,\*</sup>, Magalie Delmas<sup>2</sup>, Olivier Cerdan<sup>3</sup> & Jean-Marie Mouchel<sup>4</sup>

1: UMR G-EAU, IRSTEA, 361 rue Jean-François Breton, 34196 Montpellier Cedex 05, France -  
bruno.cheviron@irstea.fr

2: UMR LISAH, INRA, 2 place Pierre Viala, 34060 Montpellier Cedex 01, France -  
magalie.delmas@supagro.inra.fr

3: BRGM, 3 avenue Claude Guillemin, BP6009, 45060 Orléans Cedex 2, France - o.cerdan@brgm.fr

4: UMR SISYPHE, Université Paris VI-Pierre et Marie Curie, 4 place Jussieu, 75252 Paris Cedex 05,  
France - jean-marie.mouchel@upmc.fr

\* corresponding author, tel: +33 (00) 4 67 04 63 64

Keywords: River flow, sediment transport, uncertainty analysis, rating curves.

## Abstract

This paper addresses feasibility issues in the calculation of fluxes of suspended particulate matter (SPM) from degraded-quality data for flow discharge ( $Q$ ) and sediment concentration ( $C$ ) under the additional constraints of infrequent and irregular sediment concentration samplings. A crucial setting of the scope involves establishing the number of data required to counterbalance limitations in the measurement accuracy and frequency of data collection. This study also compares the merits and drawbacks of the classical rating curve ( $C=aQ^b$ ) with those of an improved rating curve approach (IRCA:  $C=aQ^b+a_1\delta S$ ) in which the correction term is an indicator of the variations in sediment storage, thus relating it to flow dynamics. This alternative formulation remedies the known systematic underestimations in the classical rating curve and correctly resists the degradation in data quality and availability, as shown in a series of problematic though realistic cases. For example, monthly concentration samplings (in average) with a random relative error in the [-30%, +30%] range combined with daily discharge records with a systematic relative error in the [-5%, +5%] range still yield SPM fluxes within factors of 0.60-1.65 of the real value, provided that 15 years of data are available. A shorter 5-day time interval (on average) between samplings lowers the relative error in the SPM fluxes to below 10%, a result directly related to the increased number of Q-C pairs available for fitting. For regional-scale applications, this study may be used to define the data quality level (uncertainty, frequency and/or number) compatible with reliable computation of river sediment fluxes. Provided that at least 200 concentration samplings are available, the use of a sediment rating curve model augmented to account for storage effects fulfils this purpose with satisfactory accuracy under real-life conditions.

## 1. Introduction

Sediment fluxes in fluvial systems reflect the denudation processes that occur on the earth's surface and exert a controlling effect on the fates of nutrients, organic pollutants and heavy metals. Therefore, assessment of sediment fluxes aids in characterising the impact of particulate transfer on water quality throughout the river system. However, the estimation of realistic sediment budgets requires long-term discharge-concentration data (Walling and Webb 1985, Ludwig and Probst 1998, Webb et al. 2003, Delmas et al. 2009), which often suffer from poor availability and reliability (Meybeck et al. 2003, Walling and Fang 2003). In particular, uncertainties in both the sampling and calculation methods affect the measurement of sediment concentration (SPM) fluxes (Rode and Surh 2007). Moreover, significant drifts in the measured quantities may arise due to the location of the sampling in the river section because the suspended sediment concentration varies within cross-sections of the rivers, thus necessitating a series of depth- and width-integrated measurements (Horowitz, 1997). However, in most cases, modellers and decision-makers use the daily discharge records combined with infrequent sediment concentration samplings, which are generally collected at a single location and exhibit high temporal variability.

Previous studies have indicated how increased sampling frequencies and total periods of data collection can reduce uncertainties in the predicted SPM or trace element fluxes (Horowitz et al. 2001, Coynel et al. 2004, Moatar and Meybeck 2005, Rode and Surh, 2007), but a complementary and perhaps broader strategy would involve treatment of the analysis in terms of the interactions between the number of data, the time interval between samplings (affected by a realistic random component) and the total period of the data collection. This analysis would be particularly pertinent in the numerous areas where available the sediment concentration data are by-products of programs for water quality monitoring that involve infrequent (approximately monthly) sampling (Delmas et al. 2012). A relevant and widely used methodology is the reconstruction of continuous (daily)

fluctuations in the sediment concentration from the empirical relationships ( $C(Q)$  rating curves) that link the sediment concentration ( $C$ ) to the water discharge ( $Q$ ) values. The classical  $C(Q)=aQ^b$  rating curve is often used for this purpose. Nevertheless, for sediment transport studies, the occasional strong non-linearity in the  $C(Q)$  relationship and the presence of only a few extreme events point to well known and problematic cases when fitting power laws (Laherrere 1996, Goldstein et al. 2004). These problematic cases suggest the use of truncated intervals of  $Q$  values (Moatar et al. 2012) or data subdivision and hypothesising of the distinct  $C(Q)$  relationships with the seasons, basin sizes or properties (Walling and Webb 1981, Smart et al. 1999, Quilbé et al. 2006; Delmas et al. 2009). Another possibility is the addition of correction terms (Laherrere and Sornette 1998) with a user-defined physical meaning. Ferguson (1986, 1987) chose the latter option in his inaugural papers that tackled the advantages and limitations in estimating sediment fluxes from power-law rating curves. Similar to other research domains, an open question is whether to attribute a deterministic physical meaning to the pre-factor and the exponent (Peters-Kümmerly 1973, Morgan 1995, Asselmann 2000) or to consider them as conceptually imperfect though demonstrably statistically relevant. Addressing these questions with a clear physical sense opens the door for a wide series of improved rating curves and variants, as advocated by Phillips et al. (1999), Asselmann (2000), Horowitz (2003) and Delmas et al. (2011), among others. For example, Picouet et al. (2001) hypothesised two sediment sources (bank and hillslope erosion), and Mano et al. (2009) introduced explicit climatic and topographic factors.

The objective of the current paper is to address the precision and sensitivity issues that exist in prediction of SPM fluxes for typical cases with data of degraded-quality gathered from infrequent samplings. We consider the  $C$  and  $Q$  measurements to be affected by errors of different types and magnitudes. As commonly reported, we hypothesised a higher probability of error for concentration than for discharge measurements. Concentration data were considered prone to random errors in a [-30%, +30%] interval around the measured values, whereas five systematic biases were tested for

discharge data in the [-20%, 20%] interval around the daily records. Moreover, infrequent concentration measurements were simulated together with slightly perturbed sampling periods. The framework of this study compares the merits and drawbacks of the classical rating curve with those of an improved rating curve approach. The latter includes a correction term as an indicator of sediment storage, thus relating the variation to flow dynamics. This work relies on a USGS dataset encompassing multiple rivers, basin typologies and years.

## 2. Material & Methods

### 2.1 Database

The present study relies on daily discharge-concentration data collected over several years at 22 USGS stations taken from the larger dataset available at <http://waterdata.usgs.gov/>. The selected stations cover a wide range of river basin typologies and sizes and are associated with specific discharge and SPM statistics (Table 1). For the Des Moines River station, we chose to split the records into two distinct periods because we observed notably large discharge variations over the first years of data collection (1961-1977) followed by rather limited variation over the most recent years (1977-2004). Several stations display notably low water levels and even close to intermittent flows under severe winter conditions (e.g., station 21, Salinas River near Spreckels), summer droughts (e.g., station 18, Kaskaskia River at Cook Mills) or both (e.g., station 7, Hocking River at Athens). [However, stations in the USGS database that exhibit complete drying or glaciations have been discarded from the analysis because they require different treatment. This choice tends to omit basins with small drainage areas, especially those that experience sharp climatic conditions. Nevertheless, various temperate to continental climates are accounted for at stations in California \(CA\), Illinois \(IL\), Iowa \(IA\), Missouri \(MI\), North Carolina \(NC\), Ohio \(OH\) and Virginia \(VA\). Another merit of sufficiently large basins for the present study is response times that are greater than the reference daily](#)

sampling period for the discharge and concentration measurements. In addition to the temporal arguments, large basins are also more integrative than smaller basins because they offer additional spatial variability with respect to the sediment sources and delivery processes combined with larger climatic variability.

[TABLE 1 ABOUT HERE]

## 2.2 Rating curves

In addition to the classical  $C=aQ^b$  rating curve (RC), different expressions and strategies have been tested and described in detail by Delmas et al. (2011). Among these, emphasis is placed in this work on the Improved Rating Curve Approach (IRCA), which hypothesises  $C=aQ^b+a_1\delta S$ , where  $a_1$  is a parameter,  $S$  is the sediment storage index and  $\delta S$  is the daily variation. This method operates in two steps. First, the method fits the  $C=aQ^b$  model, thus freezing the  $a$  and  $b$  coefficients, and subsequently fits the  $a_1$  parameter, which is the only remaining degree of freedom in the  $a_1\delta S$  correction term. The IRCA was implemented to remedy the known limitations of the RC, especially its inability to include flow dynamics or antecedent flow conditions in the prediction of  $C$  values.

For this purpose, the sediment storage index is described as a function of discharge dynamics:

$$S(t) = \exp\left(-A \frac{q(t)}{Q_0}\right) \quad [1]$$

where  $A$  is a dimensionless coefficient that controls the amplitude of  $S$  variations, and  $q(t)$  is the instantaneous  $Q(t)$  value on the rising limbs of the hydrograph or a sliding average of  $Q(t)$  values on the falling limbs. This double status of  $q(t)$  ensures asymmetry between quick sediment loading and delayed sediment storage, which is the working hypothesis that underlies the IRCA. The sliding average extends itself backwards in time towards the beginning of the current falling limb but is

limited to 20 days at most, which is the chosen approach used to account for antecedent flow conditions.

The IRCA also requires statistical analysis to establish the upper limit of the base flow, given as  $Q_0$ . From the adopted assumptions,  $S$  varies between 0 for extreme discharges (all possible sediments present in the flow) and 1 when flow ceases (all material stored and available). The choice of  $A=0.1$  yields  $S=0.95, 0.75, 0.50, 0.25$  and  $0.05$  for  $q/Q_0$  ratios of approximately 0.5, 3, 7, 14 and 30, respectively. This choice also implies that  $S \approx 0.9$  for  $q=Q_0$ , and thus the “sediment availability” would be approximately 90%.

Figure 1 shows the variations in the sediment storage index in an application to the Hocking River at Athens (station 7, Table 1). The figure displays the main characteristics of this approach: asymmetry between the delayed sediment storage and quick sediment mobilisation, damping of the high-frequency oscillations and maximum sediment storage associated with long-lasting low discharges. The intent of the IRCA is to use the daily variations of the sediment storage index as relevant information for the flow dynamics, as handled by the  $a_1 \delta S$  correction term in the  $C=aQ^b+a_1 \delta S$  model.

[FIGURE 1 ABOUT HERE]

In a strict sense, both the  $C=aQ^b+a_1 \delta S$  and  $C=aQ^b+a_1 \delta S$  expressions should be considered in this work as “models” and not “laws”. Laws should be written with an additional explicit error term, either multiplicative or additive, whose distribution should be assessed from the characteristics and is missing in the data ( $Q, C$ ) measurements. This option would take into account that the  $C=aQ^b$  and  $C=aQ^b+a_1 \delta S$  expressions are exact formulations of the problem, attributing the deviations between the calculated and observed quantities to variations in the associated error terms. Instead, the current option views the  $C=aQ^b$  and  $C=aQ^b+a_1 \delta S$  expressions as imperfect models with inherent



errors. Therefore, the scope of this work focuses on the dispersion of the model predictions with alterations of the (Q, C) dataset.

### 2.3 Fitting procedures

All fittings were automated using a multi-stage procedure centred on the PEST parameter estimation software (Doherty, 2004) but also resorted to further programming. Figure 2 displays the simplified flow chart, which is briefly described. The user selects a  $C(Q)$  model with  $p$  parameters to fit, entering the flow chart with the initial  $p_0$  vector of parameter values and also providing a series of  $Q_i$  discharge samplings. This  $(Q_i, p)$  set is processed via a program that calculates the “fitted”  $C_i^{(f)}$  value associated with each  $Q_i$  value for the selected power law. Next, PEST carries out an overall optimisation based on the minimisation of an objective function, which is calculated as the sum of the squared residuals between the observed  $C_i$  values and the fitted  $C_i^{(f)}$  values. Once the optimisation has been completed, PEST estimates the goodness-of-fit by calculating the coefficient of determination, known as  $R$ . The  $R$  value may therefore be used for comparisons between fittings. One of the interesting features in PEST is its ability to handle power laws with or without log transformations, and the choice is left to the user’s discretion. Slightly better results have been obtained in this work by fitting the untransformed expressions.

[FIGURE 2 ABOUT HERE]

### 2.4 Methods for calculating fluxes and errors

The real amount of exported sediment in the  $[0, T]$  total time period is the unknown SPM flux:

$$F = \int_0^T Q(t)C(t)dt \quad [2]$$

where  $Q$  is the discharge,  $C$  is the concentration of suspended particulate matter (SPM) and  $t$  is time.

191

192 The straightforward approximation for direct calculation of  $F$  is:

$$F_N = \sum_{i=1}^N Q_i C_i \delta t_i \quad [3]$$

193 where  $Q_i$  and  $C_i$  are time-averaged values over the  $\delta t_i$  intervals covering the  $[0, T]$  time period.

194

195 The discrepancy between  $F$  and  $F_N$  plausibly increases with increased  $\delta t_i$  values. Nevertheless, certain  
196 rare and fortuitous combinations of large  $\delta t_i$  values may still lead to  $F_N \approx F$ , from compensating  
197 effects between the underestimations and overestimations of SPM fluxes over certain periods.  
198 Therefore, the gap between  $F_N$  and  $F$  is not expected to vary in any monotonous or linear manner  
199 with increasing  $\delta t_i$  values. By contrast, the  $\delta t_i$  intervals that are smaller than the characteristic time  
200 period of fluctuations in  $Q$  and  $C$  values tend to ensure the reliability of the  $F_N$  approximation.  
201 Because the SPM regimes are related to the basin sizes (Meybeck et al. 2003) and only drainage  
202 areas larger than 1000 km<sup>2</sup> are considered in this work, the  $F_N$  fluxes calculated from the error-free  
203 daily discharge and concentration records are considered as exact solutions ( $F_N \approx F$ ) in the following.  
204 The subsequent developments aim to test the deviations from this best-case scenario that appear  
205 when coping with infrequent and/or uncertain data (i.e., random errors in the concentration data  
206 and systematic errors in the discharge data and sparse concentration samplings in this work).

207

208 The missing concentration data in [3] may be replaced by concentration values obtained from the  
209 fitted  $C(Q)$  models. Each  $Q_i$  datum results in a predicted  $C_i^{(f)}$  concentration value, and the exported  
210 SPM flux now can be approximated by:

$$F_{N,f} = \sum_{i=1}^N Q_i C_i^{(f)} \delta t_i \quad [4]$$

211

The hypothesis for the missing  $C$  data implies that only  $n < N$  values have been measured. In the calculation of  $F_{N,f}$ , one may either use the available concentration data  $C_i$  instead of the fitted values or systematically resort to the entire series of  $C_i^{(f)}$  values, as in this study.

From a theoretical point of view, any given  $C_i^{(f)}$  is an unknown function of the entire dataset via the fitting procedure:

$$C_i^{(f)} = C_i^{(f)}(Q_1, Q_2, \dots, Q_N, C_1, \dots, C_n, \Delta t_1, \dots, \Delta t_n) \quad [5]$$

with irregular  $\Delta t_k$  intervals between successive  $C$  samplings in the general case.

For regular  $\Delta t$  intervals between concentration samplings, the  $(\Delta t_1, \dots, \Delta t_k, \dots, \Delta t_n)$  temporal argument could be reduced to  $(\Delta t, n)$  or  $(\Delta t, T)$  without any additional loss of information. Combining these elements with shortened notations  $Q' = (Q_1, \dots, Q_N)$  and  $C' = (C_1, \dots, C_n)$  would yield:

$$C_i^{(f)} = C_i^{(f)}(Q, C, \Delta t, T) \quad [6]$$

The assessment of SPM fluxes ( $F_{N,f}$ ) from the source data  $(Q', C')$  under experimental conditions  $(\Delta t, T)$  is a two-stage process that first solves the inverse problem by fitting the optimal  $\{p\}$  parameter set in the  $C(Q)$  model (rating curve) and subsequently uses it for direct calculations by means of [4]:

$$(Q, C, \Delta t, T) \rightarrow \{p\} \rightarrow F_{N,f} \quad [7]$$

Most of the time, at least in the French river surveillance network, the intervals between  $C$  samplings are only approximately regular such that  $\Delta t^{\sim}$  should be used instead of  $\Delta t$ . The present procedure is assumed to be valid if the average of the  $\Delta t^{\sim}$  values over the data collection period remains sufficiently close to  $\Delta t$ . In other words, this hypothesis is intended to authorise random fluctuations of  $\Delta t^{\sim}$  around  $\Delta t = T/n$  and is not assumed to hold for drastic changes in data collection strategy.

The objective of Step 1 is to test the combined effects of systematic biases in  $Q'$  with random errors on  $C'$ , thus maintaining the optimal conditions of data collection: daily discharge and concentration data over several years. Emphasis is placed on the effects of degraded data quality on both the fitted parameters and the estimated SPM fluxes for the classical ( $C=aQ^b$ ) and improved ( $C=aQ^b+a_1\delta S$ ) rating curves.

Five systematic relative errors in the discharge measurements are addressed and are noted as  $Q_r = -20\%$ ,  $-10\%$ ,  $0\%$ ,  $+10\%$  and  $+20\%$ : if  $Q^*$  is the measured dataset and  $Q'$  is the collection of exact values, the listed  $Q_r$  cases are also written as  $Q^*/Q'=0.8, 0.9, 1.0, 1.1$  and  $1.2$ , respectively. However, random relative errors in the concentration measurements ( $C^R$ ) were assumed as uniformly distributed within the  $[-30\%, +30\%]$  interval around the collected data. This random treatment involved replicating each station in Table 1 into 100 virtual stations with the intended perturbations in the  $C$  data.

The selected objectives are to study the relative variations of the parameters  $\{p_r\}$  and those of the calculated SPM fluxes. The latter appear in more eloquent representations when displaying the ratios of calculated and exact fluxes such that the stages of the test procedure may be summarised in:

$$(Q_r, C^R) \rightarrow \{p_r\} \rightarrow F_{N,f} / F \quad [8]$$

where the expected results are the mean variation trends in function of  $Q_r$  values with dispersion effects arising from the randomised  $C^R$  concentration data. The  $\{p_r\}$  set is  $\{a_r, b_r\}$  for the classical rating curve and  $\{a_r, b_r, a_{1r}\}$  for the IRCA.

Step 2 focuses on the effects of the sampling frequencies, especially those with increasing time intervals between  $C$  data, while ensuring that the data quality is unaffected, thus producing error-free  $Q$  and  $C$  data. Numerous combinations of  $(\Delta t^R, T_c)$  values have been tested, where  $\Delta t^R$  designates an average sampling interval affected by a “small” random perturbation (at most equal to

$\Delta t/2$ ), and  $T_C$  is the total period of data collection. The  $\Delta t^R$  treatment is the approach chosen to account for the irregular  $\Delta t$  intervals previously mentioned. The targets are once again the relative variations and dispersions of the SPM fluxes, as shown in the ratios of calculated and exact fluxes:

$$(\Delta t^R, T_C) \rightarrow F_{N,f} / F \quad [9]$$

Step 3 analyses the combined effects of the degraded  $Q$ - $C$  data quality and infrequent  $C$  measurements on the calculated SPM fluxes within the following procedure:

$$(Q, C^R, \Delta t^R, T_C) \rightarrow F_{N,f} / F \quad [10]$$

Finally, step 4 provides an application of the IRCA around the estimation of SPM exports from French rivers to the sea. Contrary to the preceding sections,  $F$  is unknown and is thus estimated from “confidence intervals” around the  $F/F_{N,f}$  ratios by relying on the calculated  $F_{N,f}$  fluxes.

### 3. Results and discussion

#### 3.1 Step 1: Effects of data uncertainty on the calculated SPM fluxes

##### Effects of data uncertainty on the fitted parameters

Theoretical predictions are available from the scale-invariant properties of the  $C=aQ^b$  law: the law should still hold with a modified pre-factor ( $a^*$  instead of  $a$ ) and unchanged exponent ( $b$ ) when modifying the argument, i.e., measuring  $Q^*$  instead of the real  $Q$  value:

$$C = aQ^b = a\left(\frac{Q}{Q^*}Q^*\right)^b = a^*Q^{*b} \quad [11]$$

with  $a^*=a(Q/Q^*)^b$ .

For example, the underestimation of  $Q$  by 20% ( $Q_r = -20\%$ ) corresponds to  $Q^*/Q = 0.8$ , thus  $Q/Q^* = 1.25$  and  $a^*/a = (1.25)^b$ . A numerical application with a typical  $b$  value of 0.85 yields  $a^*/a=1.21$ . In such a case, a relative variation  $a_r = +21\%$  is theoretically expected. Similar predictions are available for the other tested  $Q_r$  values and are represented by the “Theory” dotted lines in Figure 3. Because the  $b$  exponent is supposedly unaffected, its relative variation  $b_r$  should be zero. No such prediction is available for  $a_1$  and  $a_{1r}$ .

[FIGURE 3 ABOUT HERE]

Figure 3 gathers the  $a_r$ ,  $b_r$  and  $a_{1r}$  variations; the latter is specific to the  $C=aQ^b+a_1\delta S$  model, and the former two are common with the  $C=aQ^b$  model. All curves display the global averages of  $a_r$ ,  $b_r$  or  $a_{1r}$  for the 22 stations listed in Table 1, and each one is replicated into 100 virtual stations to satisfy the

random procedure on  $C$  data. Taking the example of  $a_r$ , the upper (+) and lower (-) limits of the dispersion envelope are plotted as:

$$a_r^{\pm}(Q_r) = \frac{a^*(Q_r) \pm 1.73 \sigma_{a^*}(Q_r)}{a} = a_r(Q_r) \pm 1.73 \frac{\sigma_{a^*}(Q_r)}{a} \quad [12]$$

where  $\sigma_{a^*}$  is the standard deviation in the  $a^*$  values and all quantities are functions of  $Q_r$  except  $a$ , which is the reference value obtained for  $Q_r = 0$ . The  $\sigma_{a^*}/a$  term is a normalised standard deviation.

The 1.73 factor is usually associated with a 100%-confidence interval for uniform random distributions: once the average value (AV) and standard deviation ( $\sigma$ ) are known, the real value falls in the  $[AV - 1.73 \sigma, AV + 1.73 \sigma]$  interval. In this work, the uniform random distribution  $C^R$  results in nearly uniform random distributions of  $a^*(Q_r, C^R)$  and  $a_r(Q_r, C^R)$  values for each  $Q_r$  value, thus ensuring the validity of the calculated dispersion envelope for  $a_r(Q_r, C^R)$ . The same procedure applies to parameters  $b$  and  $a_1$ .

Figures 3a, d and g examine the  $a_r(Q_r)$  trends and compare them with the theoretical predictions for increasing values of the PEST coefficient of determination ( $R$ ). The atypical non-monotonous variation displayed in Figure 3a is essentially due to poorly fitted data ( $R \approx 0.2$ ) from stations 14, 16, 18 and 19 in Table 1. At such low  $R$  values, equifinality unavoidably exists such that completely different  $(a, b)$  couples lead to similar performances in the optimisation. For the cited stations, unexpectedly high  $a$  values compensate for the effects of notably low  $b \ll 1$  values, yielding  $R$  values otherwise obtained from  $(a, b)$  couples with  $b \approx 1$ .

In Figure 3a, d and g, the dispersion decreases with increasing  $R$  values and remains limited in the sense that variability is explained by the  $a_r(Q_r)$  trends rather than by the “orthogonal” dispersive random effects. As expected, the  $a_r(Q_r)$  curves best match the theoretical curves for increasing  $R$

values, which indicate a clearer power-law organisation of the dataset. Unfortunately, only 7 stations are encompassed by the  $R>0.65$  criteria vs. 17 stations out of 22 for  $R>0.3$ .

Rather weak dispersions and low  $b_r$  values (i.e., nearly unchanged  $b$  exponents) in Figure 3b, e, and h appear to be in good agreement with expectations arising from the scale-invariance properties of power laws. However, a striking feature is the increasing variability of  $a_r$  and  $b_r$  with decreasing determination values. The underlying and unanswered question at this point is whether this variability will endanger the reliability of SPM flux calculations for fittings with low determination values. This question is the subject of the advocated “composite analysis” performed in the following paragraphs, from data uncertainty to uncertainty in the fitted parameters as well as in the calculated fluxes.

The  $a_{1r}$  variations (Figure 3c, f and i) also show limited dispersion, except for strong discharge underestimations. Positive relative errors in the discharge ( $Q_r>0$ ) cause positive relative variations in the  $a_1$  coefficient ( $a_{1r}>0$ ). A key point is that the  $\delta S$  term is identical regardless of the  $Q_r$  value because the  $q/Q_0$  ratio is used in [1], where both  $q$  and  $Q_0$  are affected by the same relative error in the discharge values. This choice of  $\delta S$ , referred to as “identical by construction”, allows direct interpretation of the role played by  $a_1$ : the  $a_1\delta S$  correction behaves similar to  $a_1$ , producing its strongest relative variations ( $a_{1r}=-30\%$ ) for the strongest discharge underestimations ( $Q_r=-20\%$ ).

#### *Effects of data uncertainty on the calculated SPM fluxes*

Contrary to the fitted coefficients, the calculated SPM fluxes exhibit almost no dependence on the determination ( $R$ ) values. Therefore, Figure 4 plots the SPM fluxes and dispersions obtained for all  $R$  values. As shown previously, the upper (+) and lower (-) limits of the dispersion envelope are written:



$$\left(\frac{F_{N,f}}{F}\right)^{\pm}(Q_r) = \frac{F_{N,f}(Q_r) \pm 1.7 \sigma_{F_{N,f}}(Q_r)}{F} = \left(\frac{F_{N,f}}{F}\right)(Q_r) \pm 1.7 \frac{\sigma_{F_{N,f}}(Q_r)}{F} \quad [13]$$

[FIGURE 4 ABOUT HERE]

Figure 4a and b show weak dispersions and similar variation trends because the calculated SPM fluxes increase with the estimated discharge values. The relative variations in the calculated fluxes are near-linear functions of the systematic relative error present in the discharge measurements for both the classical  $C=aQ^b$  (Figure 4a) and the improved  $C=aQ^b+a_1\delta S$  (Figure 4b) rating curves. The difference between these parallel curves is the “offset” added in Figure 4b by the  $a_1\delta S$  correction, which perfectly remedies the underestimation due to the classical method. The gain obtained from the  $a_1\delta S$  correction is approximately 5% along the “calculated on exact” vertical axis, with even weaker dispersion in the results. For example, if the discharge is known with a 10% uncertainty (5% on each side of the  $Q_r=0$  line), then  $F_{N,f}/F$  lies within the 0.88-1.04 and 0.93-1.07 ranges of the classical and improved rating curves, respectively.

Looking at the nearly stable  $b$  values ( $b_r \approx 0$  in Figure 3b, e and h), it is worth noting that increases in the fitted  $a$  values ( $a_r > 0$  in Figure 3d and g) were not sufficient to counterbalance the influence of the discharge underestimations ( $Q_r < 0$ ). The calculated fluxes still underestimate the real values when the discharge is underestimated for both methods in Figure 4. However, the overall effect of the storage term is an increase in the calculated ( $F_{N,f}$ ) SPM fluxes, which is validated by improvements of approximately 5% in the determination values.

### 3.2 Step 2: Effects of data infrequency on the calculated SPM fluxes

This subsection leaves data quality concerns aside to focus on data availability, especially on the problem of infrequent  $C$  data. This subsection also tackles the sampling frequency issue by addressing the interplay between the number ( $n$ ) of available data, the total collection period ( $T$ ) and the sampling period ( $\Delta t$ ), as commented next to [6]. As previously mentioned, the sampling periods have always been tested with slight random perturbations ( $\Delta t^R$ ) of the predefined values to account for more realistic field conditions, resulting in approximations ( $\Delta t^{\sim}$ ) of the predefined  $\Delta t$  intervals. Figure 5 displays the ratio of the calculated and exact SPM fluxes, the medians of the absolute errors on this ratio and the statistics for the absolute errors on this ratio in the  $\Delta t^{\sim}30$  day case for various ( $n, T, \Delta t$ ) triplets, thus allowing comparisons between the fitted  $C=aQ^b$  and  $C=aQ^b+a_1\delta S$  models.

[FIGURE 5 ABOUT HERE]

Figure 5a targets the evolution of the “calculated on exact” ratios of SPM fluxes for decreasing values of the sampling interval ( $\Delta t$ ) and also shows the positive impact of increasingly long periods of data collection ( $T$ ) for the given sampling intervals. A clear increase in dispersion occurs for  $\Delta t > 5$  days combined with  $T < 4$  years. Further on the left of the diagram, the rather typical monthly sampling period ( $\Delta t^{\sim}30$  days) requires at least an 8-year collection period ( $T=8$  years) for the “calculated on exact” ratios to lie within the gross [0.5, 5.0] interval. Figure 5b also begins with highly dispersed values for combinations of high sampling periods, even with long collection periods, and exhibits additional oscillations before achieving convergence because it is obviously more seriously affected by weak  $T$  values. The main difference is the highest dispersion for  $\Delta t^{\sim}5$  days and  $T=4$  years and for  $\Delta t^{\sim}20$  days and  $T=8$  years. A common point appears to be the trend of overestimating the exact SPM fluxes, even for the most relevant estimations that rely on low  $\Delta t$  and high  $T$  values.

A complementary view is given by Figure 5c and d and shows the median of the absolute error of the calculated against exact ratio as a function of the number of available concentration data ( $n$ ) by

plotting a dedicated curve for each of the total tested collection periods ( $T=1, 4, 8, 12$  and  $15$  years). Figure 5c shows that  $n=150$  takes the error under  $20\%$ , whereas  $n=300$  is required for errors lower than  $10\%$ . These results are nearly independent of  $T$  and thus hold for sampling intervals  $\Delta t=T/n$  with  $n$  above the mentioned thresholds. For example, it takes  $\Delta t \sim 20$  days for  $T=8$  years to dispose of  $n=150$  concentration data. Equivalently,  $T=13.7$  years is the minimum time period required to fulfil the  $20\%$  error criterion when performing monthly samplings ( $\Delta t \sim 30$  days). By contrast, the trends in Figure 5d are less uniform because the error values exhibit a clear dependence on the  $T$  values, which calls in question analyses that only involve the number  $n$  of concentration data and make a case for combined  $(n, T)$  criteria. For example,  $n > 200$  and  $T \geq 8$  years will confine the relative error to under the  $20\%$  mark. For monthly samplings, the  $n > 200$  threshold alone corresponds to  $T > 18$  years, which *de facto* verifies  $T \geq 8$  years. This result tends to indicate that the condition for the number of data remains the most restrictive and could still be maintained alone.

Figures 5e and f focus on the case of monthly concentration samplings. The monotonic and exponential-like decrease of the error in Figure 5e emphasises the regular gain in the stability of the  $C=aQ^b$  method for total data collection periods increasing from  $T=1$  to  $15$  years. Figure 5f shows the same trend with a few irregularities. The dynamic definition chosen for the storage term ( $S$ ) and its variations ( $\delta S$ ) plausibly requires sufficiently dense concentration data for significant gains in precision, with potentially better performances than the  $C=aQ^b$  method but apparently with slightly more restrictive conditions of application.

### 3.3 Step 3: Combined effects of data uncertainty and infrequency on the calculated SPM fluxes

Subsection 3.1 established the ability of the  $C=aQ^b+a_1\delta S$  model to better predict the SPM fluxes, as compared with the  $C=aQ^b$  model, using degraded-quality data. Subsection 3.2 showed that the  $C=aQ^b+a_1\delta S$  model was slightly more sensitive to data infrequency. The present subsection tests both

models against combined data uncertainty and infrequency to simulate eventual real-life conditions: systematic relative errors in the discharge measurements (poorly-gauged stations), random errors in the concentration measurements (uncertain techniques) and possibly sparse concentration measurements (limited credits).

Figure 6 uses the 100%-confidence intervals, similar to these already defined in [12] and [13], to draw dispersion envelopes associated with the random treatment of concentration data for daily ( $\Delta t \sim 1$  day), decadal ( $\Delta t \sim 10$  days) and monthly ( $\Delta t \sim 30$  days) concentration samplings. The  $\Delta t \sim 1$  day case corresponds to the results shown in Figure 4. In Figure 6, sparser concentration samplings lead to wider dispersion envelopes that are somewhat shifted towards higher flux predictions. The drift and dispersion are a bit more pronounced for the storage method with too many data lacking, although the curves are quite similar between sketches (a) and (b). Figure 6 also proves that infrequent and limited-quality data may still be used for flux predictions (at least with caution and while staying within the tested ranges for errors) because they do not lead to completely divergent, uncontrolled or unpredictable results.

[FIGURE 6 ABOUT HERE]

As a mean behaviour among all stations, if one commits a systematic relative error within the [-5%, +5%] interval on  $Q$  together with a random relative error within the [-30%, +30%] interval on  $C$  while only disposing of  $C$  data each 30 days on average, the calculated SPM flux still lies within a factor of 0.60-1.60 of the real value with the classical rating curve. The improved rating curve gives the estimation in the 0.65-1.65 range. A narrower 0.80-1.40 range would be obtained if considering 60%-confidence intervals instead of 100%-confidence intervals. The following subsection therefore addresses possible applications in bounding sediment budgets.

### 3.4 Step 4: Application to sediment exports from French rivers

In real-life situations, the predicted flux is known, and the objective is to define a plausible interval for the real flux. This process may be carried out by examining the “exact against calculated” ratios along the y-axis instead of the “calculated against exact” ratios shown in the previous figures. Figure 7a presents dispersion envelopes corresponding to the 100%-confidence intervals, indicating where the exact SPM flux may lie for sampling periods of  $\Delta t \sim 10$  days and  $\Delta t \sim 30$  days. Taking a 10% uncertainty for the discharge measurements (between -5 and +5%), retaining the 60% random uncertainty in the concentration data (between -30% and +30%) and assuming a worst-case sampling interval of  $\Delta t \sim 30$  days for the concentration data, the real flux ( $F$ ) lies between 0.6 and 1.53 times the calculated value ( $F_{N,r}$ ).

In the French sediment budget proposed by Delmas et al. (2012) for the major rivers to the sea, the calculations were performed from monthly sediment concentration samplings ( $\Delta t \sim 30$  days) over more than 25 years, except for the Rhone river, for which daily measurements were available in certain periods, yielding an average of  $\Delta t \sim 10$  days. Figure 7b shows the induced uncertainty in the calculated sediment fluxes. The estimated total sediment load for the selected rivers is 13.9 Mt/yr. From the uncertainties calculated in this work, the real sediment export from these rivers is contained between 10.05 Mt/yr and 17.7 Mt/yr.

[FIGURE 7 ABOUT HERE]

#### 4. Conclusion

This paper tackled feasibility and precision issues in calculation of fluxes of suspended particulate matter (SPM) by assuming systematic errors in the water discharge ( $Q$ ) and random errors in sediment concentration ( $C$ ) data and under the additional constraint of infrequent sediment concentration samplings. The chosen framework compared the merits and drawbacks of the classical rating curve ( $C=aQ^b$ ) with those of an improved rating curve approach (IRCA,  $C=aQ^b+a_1\delta S$ ) in which the correction term is an indicator of the variations in sediment storage and is thus related to flow dynamics. Successive steps of the analysis were: (1) to establish the effects of data uncertainty on the fitted coefficients ( $a$ ,  $b$ ,  $a_1$ ) and on the calculated SPM fluxes, (2) to examine how infrequent sediment concentration data affects these estimates and (3) to combine both effects into the definition of realistic cases, thus allowing an application to sediment exports from French rivers.

Step 1 involved systematic relative errors in the flow discharge (-20%, -10%, 0%, +10%, +20%) and random relative errors in the sediment concentration in the [-30%, +30%] interval. Increasing  $a$  values and stable  $b$  values were observed when gradually moving from -20% to +20% errors in the discharge, together with decreasing dispersion in the fitted ( $a$ ,  $b$ ) coefficients with the increasing goodness-of-fit. Such results globally meet the expectations arising from the scale-invariant properties of power laws. As a complement, the dispersion in the magnitude of the  $a_1\delta S$  correction term appeared far stronger for the most severe discharge underestimations than for all other tested errors. The general trend was that of an upward correction due to the  $a_1\delta S$  term: the IRCA remedies the small systematic underestimations observed with the classical rating curve method. [The IRCA always performs better than the classical rating curve \(and does not require additional information\) when frequent concentration measurements are available, regardless of the period of data collection and the tested errors in the discharge and concentration.](#)

Step 2 hypothesised error-free discharge and concentration measurements to focus on the effects of sampling frequencies on the calculated sediment fluxes. The results show that the number ( $n$ ) of available C measurements is more discriminating than the sampling frequency itself, at least within the tested data collection strategies, and the provided data measurements captured sufficient variability in the river behaviour according to the Wilcoxon test of data representativity. The criteria on  $n$  were revealed as the most restrictive with respect to the performances of the rating curves:  $n > 200$  guaranteed that the calculated SPM fluxes would lie within the  $[-20\%, +20\%]$  interval around the exact values.

Step 3 consisted of combining the previous aspects and checking whether degradation of the results remained progressive and controlled, or if data uncertainty and infrequency would yield diverging results and render the methods inapplicable. This question was especially pertinent for the IRCA, that was slightly better in dealing with uncertain data but was slightly more sensitive to data infrequency. Bounding the calculated SPM fluxes within the confidence intervals around the real values allowed the following observations: the calculations are slightly higher with the improved rating curve, and the dispersion also grows slightly wider with increasing errors in discharge, but the results always stay within the acceptable margins of errors.

In the chosen worst-case scenario, poor sampling intervals of 30 days (on average) over approximately fifteen years combined with relative errors in discharge between  $-5\%$  and  $+5\%$  and random errors within the  $[-30\%, +30\%]$  interval for the sediment concentration values resulted in calculated fluxes that are still bounded within a factor of 0.60 to 1.65 of the real values. However, all other realistic cases yield far better estimates. For example, there is no technical improvement, but a shorter 5-day sampling interval on average reduces the relative error to below 10%. Finally, the application to French rivers illustrated the reliability of the method for a wide variety of irregular sampling intervals and flow discharge and sediment concentration ranges, provided that sufficient

concentration data were available. In addition to technical improvements, a key issue is to better address the irregular samplings and thus to extract additional information from the discharge dynamics, especially the antecedent flow conditions, through ongoing developments around the sediment storage term in the IRCA.

In its present formulation, the IRCA perfectly corrects the known underestimation of the classical rating curve, if frequent concentration samplings are available, combined with the uncertainties of discharge and concentration values. Both methods perform well when concentration samplings become sparse if the sampling period and number of concentrations remain sufficiently large. Finally, only the IRCA is subject to improvements for better exploitation of the information contained in the temporal dynamics of discharge.

#### **Acknowledgment**

The authors would like to acknowledge the financial support of the PIREN Seine Program and the support and constructive comments of Xavier Bourrain and Jean-Noel Gautier of the AELB.



## References

- Asselmann, N. E. M., 2000. Fitting and interpretation of sediment rating curves, *Journal of Hydrology*, 234, pp.228-248.
- Clauset, A., Shalizi, C. R., Newman, M. E. J., 2009. Power-law distribution in empirical data, *Society for Industrial and Applied Mathematics – Review*, 51 (4), pp.661-703.
- Coynel, A., Schäfer, J. Hurtrez, J. E., Dumas, J., Etcheber, H., Blanc, G., 2004. Sampling frequency and accuracy of SPM flux estimates in two contrasted drainage basins. *Science of the Total Environment* 330, pp.233–247.
- Delmas, M., Cerdan, O., Mouchel, J. M., Garcin, M., 2009. A method for developing large-scale sediment yield index for European river basins, *Journals of Soils and Sediments*, 9 (6), pp.613-626.
- Delmas, M., Cerdan, O., Cheviron, B., Mouchel, J.-M., 2011. River basin sediment flux assessments, *Hydrological Processes*, 25 (10), pp.1587-1596.
- Delmas, M., Cerdan, O., Cheviron, B., Mouchel, J.-M., Eyrolle, F., 2012. Sediment exports of French rivers to the sea, *Earth Surface Processes and Landforms*, 37 (7), pp.754-762.
- Doherty, J., (2004). PEST – Model-independent parameter estimation, User Manual, Watermark Numerical Computing.
- Ferguson, R. I., 1986. River loads underestimated by rating curves, *Water Resources Research*, 22 (1), pp.74-76.

560

561 Ferguson, R. I., 1987. Accuracy and precision of methods for estimating river loads, *Earth Surface*  
562 *Processes and Landforms*, 12 (1), pp.95-104.

563

564 Goldstein, M. L., Morris, S. A., Yen, G. G., 2004, Problems with fitting to the power law distribution,  
565 *European Physical Journal B*, 41 (2), pp.255-258.

566

567 Horowitz, A. J., 1997. Some thoughts on problems with various samplings media used for  
568 environmental monitoring, *Analyst*, 122, pp.1193-1200.

569

570 [Horowitz, A. J., Elrick, K. A. and Smith, J. J., 2001. Estimating suspended sediment and trace element](#)  
571 [fluxes in large river basins: methodological considerations as applied to the NASQAN programme,](#)  
572 [Hydrological Processes](#), 15, pp.1107-1132.

573

574 Horowitz, A. J., 2003. An evaluation of sediment rating curves for estimating suspended sediment  
575 concentration for subsequent flux calculation, *Hydrological Processes*, 17, pp.3387-3409.

576

577 Laherrere, J., 1996. "Parabolic fractal" distributions in nature, *Comptes-Rendus de l'Académie des*  
578 *Sciences – 2A Sciences de la Terre et des Planètes*, 322 (7), pp.535-541.

579

580 Laherrere, J., Sornette, D., 1998. Stretched exponential distributions in nature and economy: "fat  
581 tails" with characteristic scales, *European Physical Journal B*, 2 (4), pp.525-539.

582

583 Ludwig, W., Probst, J. L., 1998. River sediment discharge to the oceans: present-day controls and  
584 global budgets, *American Journal of Science*, 298, pp.265-295.

585

Mano, V., Nemery, J., Belleudy, P. and Poiriel, A., 2009. Assessment of suspended sediment transport in four alpine watersheds (France): influence of the climatic regime, *Hydrological Processes*, 23, pp.777-792.

Meybeck, M., Laroche, L., Durr, H. H. and Syvitski, J. P. M., 2003. Global variability of daily total suspended solids and their fluxes in rivers, *Global and Planetary Change*, 39, pp.65-93.

Mitzenmacher, M., 2004. A Brief history of generative models for power law and lognormal distributions, *Internet Mathematics*, 1 (2), pp.226-251.

Moatar, F., Meybeck, M., Raymond, S., Birgand, F., Curie, F. (2012). River flux uncertainties predicted by hydrological variability and riverine material behavior, *Hydrological Processes*, DOI: 10.1002/hyp.9464.

Moatar, F., Meybeck, M., 2005. Compared performance of different algorithms for estimating annual loads flows by the eutrophic River Loire, *Hydrological Processes*, 19, pp.429-444.

Morgan, R.P.C., 1995. Soil erosion and conservation, 2nd ed., Longman, London.

Newman, M. E. J., 2005. Power laws, Pareto distributions and Zipf's law, *Contemporary Physics*, 46 (5), pp.323-351.

Peters-Kümmerly, B.E., 1973. Untersuchungen über Zusammensetzung und Transport von Schwebstoffen in einigen Schweizer Flüssen, *Geographica Helvetica*, 28, pp.137–151.

Phillips, J. M., Webb, B. W., Walling, D. E., Leeks, G. J. L., 1999. Estimating the suspended sediment loads of rivers in the LOIS study area using infrequent samples, *Hydrological Processes*, 13, pp.1035-1050.

Picouet, C., Hingray, B. and Olivry, J. C., 2001. Empirical and conceptual modeling of the suspended sediment dynamics in a large tropical African river: the Upper Niger river basin, *Journal of Hydrology*, 250, pp.19-39.

Quilbé, R., Rousseau, A. N., Duchemin, A., Poulin, A., Gangbazo, G., Villeneuve, J. P., 2006. Selecting a calculation method to estimate sediment and nutrient loads in streams: application to the Beaurivage River (Québec, Canada), *Journal of Hydrology*, 326, pp.295-310.

Rode, M., Suhr, U., 2007. Uncertainties in selected river quality data. *Hydrol. Earth Syst. Sci.*, 11, pp.863-874.

Smart, T. S., Hirst, D. J. and Elston, D. A., 1999. Methods for estimating loads transported by rivers, *Hydrology and Earth System Sciences*, 3 (2), pp.295-303.

Sornette, D., 2006, *Critical Phenomena in Natural Sciences: chaos, fractals, self-organization and disorder* (Springer, Berlin), chapter 14, 2<sup>nd</sup> edition, 444p.

Walling, D. E., Webb, B. W., 1981. The reliability of suspended sediment load data, In *Erosion and Sediment Transport Measurement*, IAHS Publication No 133, IAHS Press: Wallingford; pp.177-194.

Walling, D. E., Webb, B. W., 1985. Estimating the discharge of contaminants to coastal rivers: some cautionary comments, *Marine Pollution Bulletin*, 16, pp.488-492.

637

638 Walling, D. E., Fang, D., 2003. Recent trends in the suspended sediment loads of the World's rivers,  
639 *Global and Planetary Change*, 39, pp.111-126.

640

641

**Table caption**

Table 1 – Names and locations of the USGS stations used in this study together with the drained areas of the monitored rivers and statistics of their discharge (Q) and concentration (C) values. The  $Q_0$  base-flow limit is an indicator introduced in the IRCA-Improved Rating Curve Approach, and  $\sigma(Q)$  and  $\sigma(C)$  report the standard deviations of the Q and C data, respectively.

650 **Table 1**  
651

USGS station	Drained area	Min Q	Base-flow Q <sub>0</sub>	Median Q	Mean Q	Max Q	σ(Q)	Min C	Median C	Mean C	Max C	σ(C)
# River name and station location	km <sup>2</sup>	m <sup>3</sup> s <sup>-1</sup>						g L <sup>-1</sup>				
1 Rappahannock River at Remington, VA	1603	0.1	17.4	11.2	19.0	1296.9	32.9	1	11	39	2070	105
2 Roanoke River at Randolph, VA	7682	5.1	72.6	49.6	79.3	1996.3	102.1	1	34	76	2060	142
3 Dan River at Paces, VA	6700	6.9	64.4	53.2	77.7	1795.3	91.6	5	60	122	2260	193
4 Yadkin River at Yadkin College, NC	5905	9.3	68.7	62.3	83.7	1868.9	87.0	1	70	150	2970	224
5 Muskingum River at Dresden, OH	15522	13.0	89.1	93.2	165.7	1067.5	177.5	1	30	60	1600	84
6 Muskingum River at McConnelsville, OH	19223	16.1	111.7	171.0	256.6	1350.0	229.7	2	48	77	1710	100
7 Hocking River at Athens, OH	2442	0.7	24.3	9.3	25.0	883.5	49.3	1	14	56	1320	116
8 Scioto River at Highby, OH	13289	7.1	121.6	61.2	133.3	3596.2	196.8	1	41	99	2520	177
9 Little Miami River at Milford, OH	3116	1.5	39.8	17.4	38.6	863.7	59.4	1	40	103	4850	216
10 Great Miami River at Sydney, OH	1401	0.8	10.0	6.7	15.9	250.3	23.6	1	50	72	1710	98
11 Stillwater River at Pleasant Hill, OH	1303	0.3	14.5	4.0	12.2	373.8	25.6	1	23	52	1970	108
12 Maume River at Waterville, OH	16395	0.5	95.0	53.0	148.6	3199.8	247.7	1	39	82	2240	129
13 Upper Iowa River near Dorchester, IA	1994	2.2	9.1	7.4	12.7	268.2	17.5	1	43	192	10000	677
14 Iowa River at Iowa City, IA	8472	1.4	21.2	37.9	64.0	410.6	65.2	1	55	103	7540	215
15 Des Moines River near Saylorville, IA	15128	0.4	44.9	27.8	69.8	1333.7	109.6	1	120	240	5400	356
16 Des Moines River near Saylorville, IA	15128	2.1	53.4	48.4	101.1	1254.4	129.4	0.7	32	46	1210	51
17 Illinois River at valley City, IL	69264	37.7	3.6	549.3	743.0	3398.0	572.3	13	120	182	3720	202
18 Kaskakia River at Cooks Mills, IL	1225	0.0†	5.8	4.9	12.7	274.4	22.8	1	46	60	1710	67
19 Kaskakia River near Venedy Station, IL	11378	2.0	35.8	53.8	109.3	1379.0	145.5	5	81	124	2590	157
20 Mississippi River at St. Louis, MO	1805222	1166.7	3808.6	4898.8	6154.1	29732.7	3841.3	21	217	340	6720	375
21 Salinas River near Spreckels, CA	10764	0.0‡	16.4	0.2	9.3	1121.3	42.6	1	36	306	24000	1273
22 Sacramento River at Sacramento, CA	60883	112.4	358.2	461.6	656.7	2797.7	495.7	8	47	75	1960	88

† Min Q=0.001 m<sup>3</sup> s<sup>-1</sup>

‡ Min Q=0.01 m<sup>3</sup> s<sup>-1</sup>

## Figure captions

Figure 1 – Sediment storage index  $S(t)$  calculated from discharge values  $Q(t)$  and  $Q_0$ , in an application to the Hocking River at Athens, Ohio (station 7, Table 1).

Figure 2 – Simplified flow chart of the fitting procedure.

Figure 3 – Relative variation and dispersion of the fitted coefficients in  $C=aQ^b$  (a, b, d, e, g, h) and  $C=aQ^b+a_1\delta S$  models (c, f, i) for increasing values of the coefficient of determination. Dispersion envelopes correspond to the 100% confidence intervals. Lines in the middle of the envelopes show averages over all stations listed in Table 1.

Figure 4 – Ratios and dispersion of calculated on exact SPM fluxes obtained from the fitted  $C=aQ^b$  (a) and  $C=aQ^b+a_1\delta S$  models (b) without any criterion for the coefficient of determination. These results were obtained from daily samplings over the entire sampling periods at each USGS station, *i.e.*, station-specific time periods. Dispersion envelopes correspond to the 100% confidence intervals. Lines in the middle of the envelopes show the averages over all stations listed in Table 1.

Figure 5 – Ratios of calculated on exact SPM fluxes (a, b), medians of the absolute errors of these ratios (c, d) and statistics for the absolute errors of these ratios for sampling periods  $\Delta t \sim 30$  days (e, f). The results are obtained from the fitted  $C=aQ^b$  and  $C=aQ^b+a_1\delta S$  models for various combinations involving the number (n) of available concentration data, the total time period for data collection (T) and the sampling period ( $\Delta t$ ) for concentration data.

Figure 6 – Dispersion envelopes for the ratios of calculated and exact SPM fluxes obtained from uncertain and infrequent concentration data by fitting  $C=aQ^b$  (a) and  $C=aQ^b+a_1\delta S$  models (b). These



results were obtained over the entire [sampling period at each USGS station, i.e., station-specific time periods](#). These dispersion envelopes correspond to the 100% confidence intervals averaged over the entire dataset listed in Table 1. Each station has been affected with systematic errors in discharge, random errors in concentration, and increased sampling periods.

Figure 7 – Dispersion envelopes (100% confidence intervals) for the ratios of exact on calculated SPM fluxes obtained from uncertain and infrequent concentration data by fitting the  $C=aQ^b+a_1\delta S$  [model](#) (a). Application to sediment exports from French rivers, where inner and outer circles bound the real SPM values (b).

## List of Figures

Figure 1:

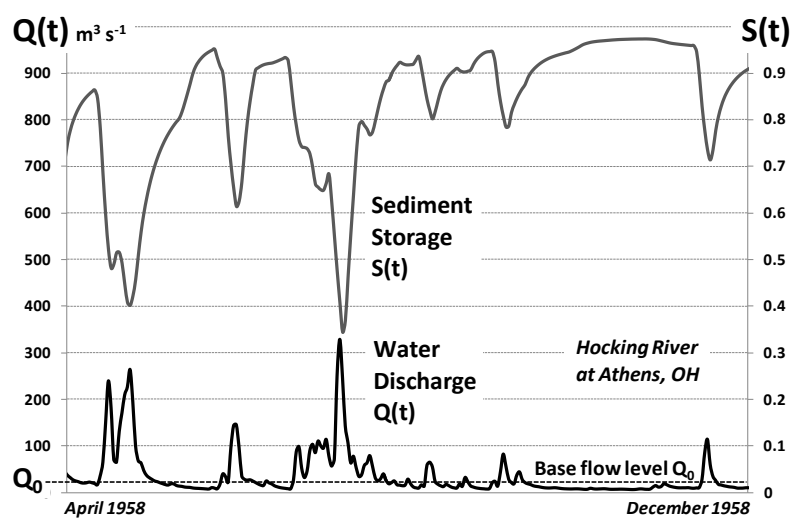


Figure 2:

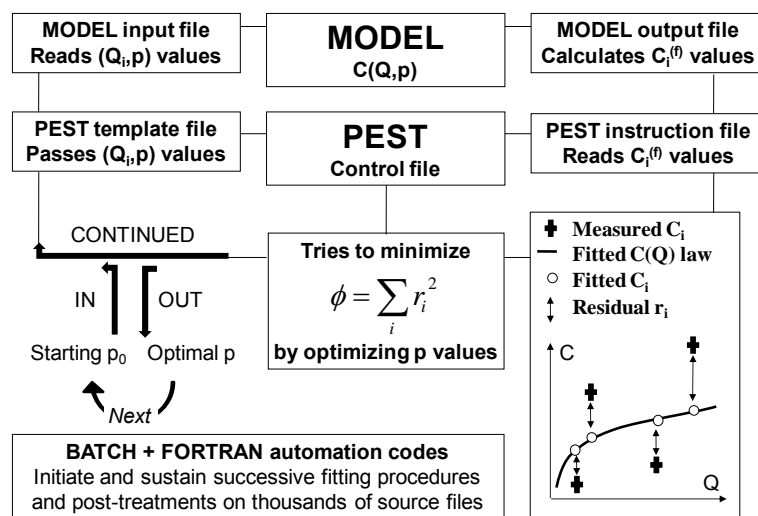


Figure 3:

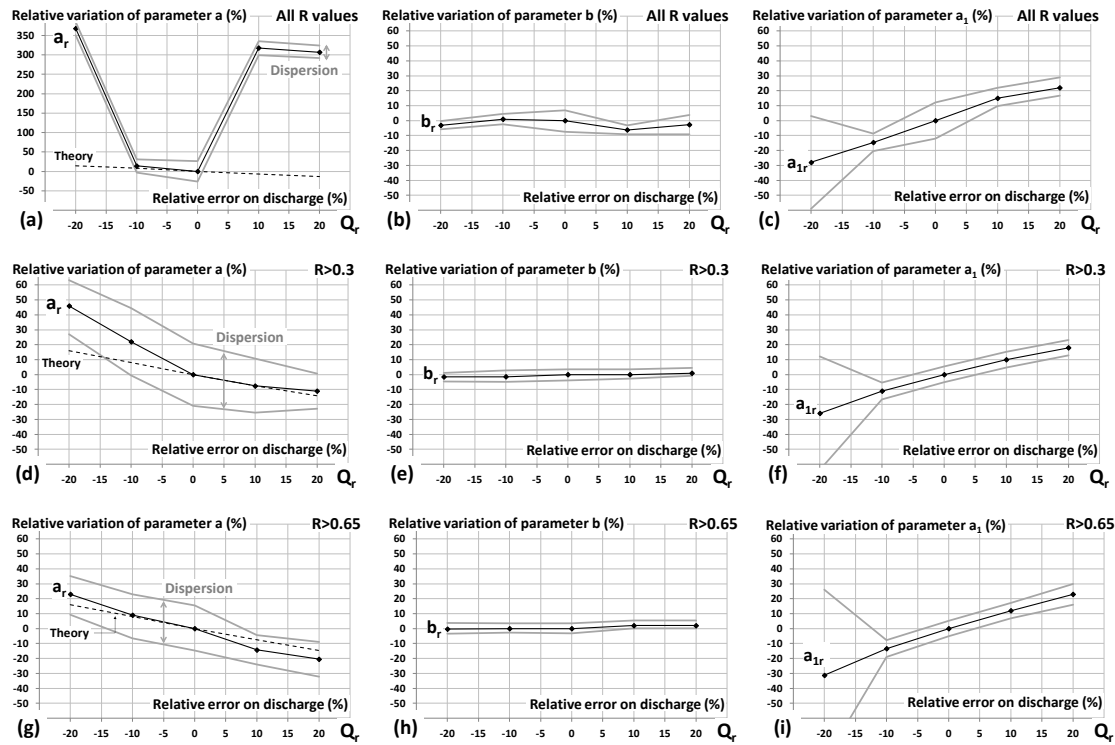


Figure 4:

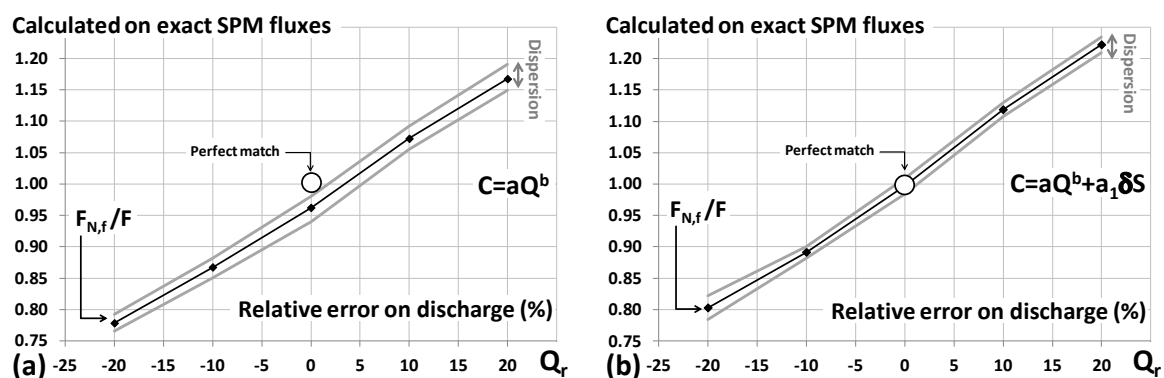


Figure 5:

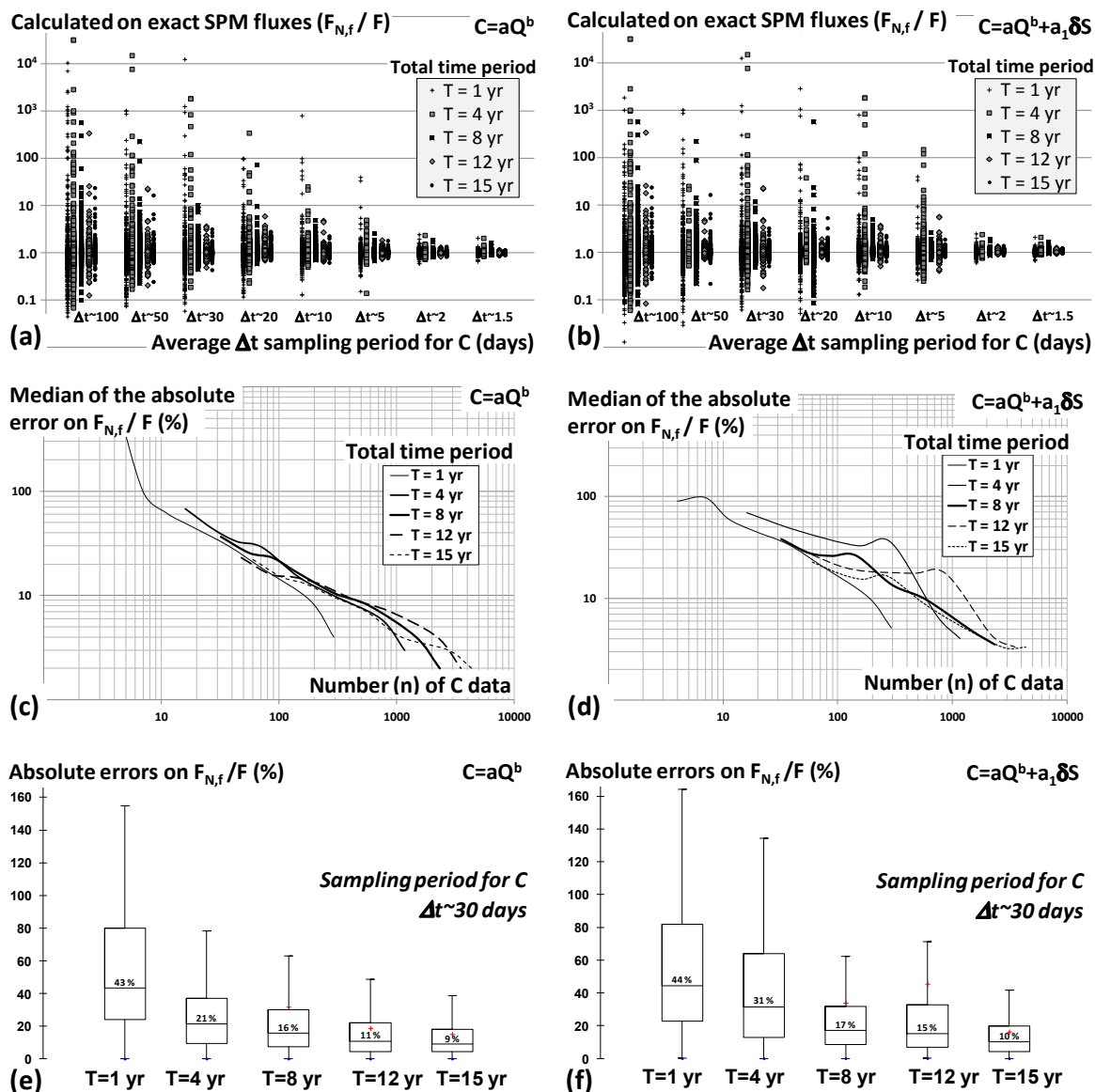


Figure 6:

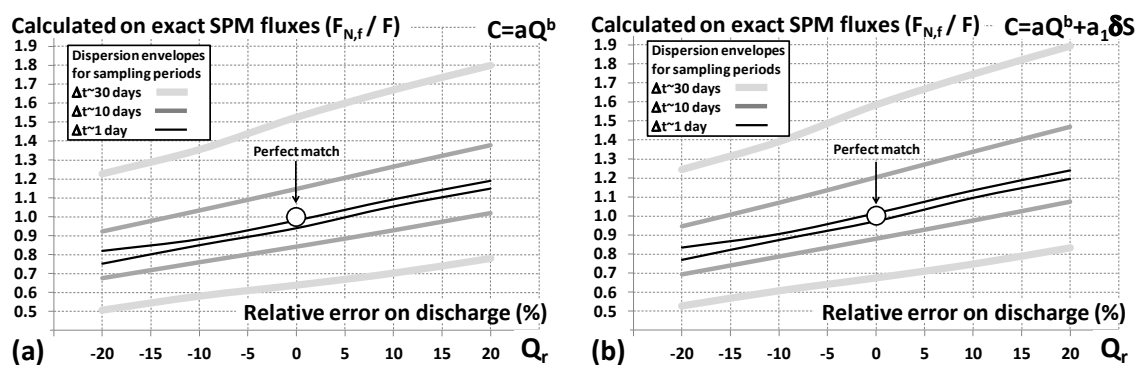


Figure 7:

